MODULAR ELECTRONIC TURBOJET CONTROL SYSTEM BASED ON TPR

Károly BENEDA*
AEROK Aviation Technical Training Centre Ltd. H1107 Budapest, Somfa köz 12., HUNGARY
*karoly.beneda@aerok.hu

Summary. Gas turbine engines are spread throughout the aviation industry due to their favourable power density and relative simplicity over reciprocating engines. In order to increase propulsive efficiency, the engine can be equipped with a fan that is delivering a large but slow airflow similarly to propellers. This group of gas turbine engines is called turbofan that is the most thoroughly utilized device for propulsion of large aircraft nowadays. Although single stream turbojet engines have less efficiency and therefore their role in commercial aviation has decreased, still they have some applications in the range of micro scale gas turbines. The control of the engine – let it be of any of the previously mentioned type – is inevitable for the proper use. Therefore accurate, fast, automatic and fault tolerant control systems are an important part of the powerplant. This article has the main goal to investigate the possibility of creating a control system for a turbojet engine based on the Turbofan Power Ratio (TPR) parameter independently of the current practice, where it is only an adjusting factor for a conventional rotor speed control. This paper focuses on the behaviour of the gas turbine with such a system implementing this novel approach and presents measurement results from ground test bench experiments, which has shown fair match between the thrust generated and TPR making it suitable for using it as a thrust parameter.

Keywords: gas turbine engine; turbojet engine; gas turbine control; FADEC; TPR; turbofan power ratio; modular electronic control

1. INTRODUCTION

Nowadays both civil and military aviation relies highly on gas turbine engines. They have gained an enormous share in the propulsion systems throughout the 1940's and 50's, when the elementary researches have acquired the necessary knowledge about their thermodynamic behaviour, structural concepts and operational circumstances. There have been developed several major groups, such as the original turbojet configuration, which has been converted later to turbofan in order to reach fair propulsive efficiency, or the turboprop version to drive smaller aircraft with a moderate speed.

In the present article, the turbojet engines are considered due to their relative simplicity in comparison with the other groups of gas turbine engines. Although their spread in the industry is constantly decreasing, there are still some applications, where these engines are used, eg radio controlled model aircraft [18] even for hobbyist usage [11], small unmanned aerial vehicles for high altitudes as well as velocities [2], [22], or auxiliary propulsion system for sailplanes [17]. These units are typical micro turbines, generating an equivalent thrust near or less than 1kN. The longitudinal section of a typical micro gas turbine engine is shown on Figure 1.

It is important to mention that similar units are also widely used for power generation where small weight, flexibility, low maintenance is required, eg backup power source for medical purposes, fire-fighting equipment, etc. [12].

Regardless of the field of usage, the safety of the flight is an essential factor that must be considered with the propulsion system as well. Therefore the control of the gas turbine engine is inevitable. It should also provide high reliability, relative simplicity and low maintenance costs due to effective fault isolation [10]. This paper guides the reader through the development of a simple electronic control for such a turbojet engine.

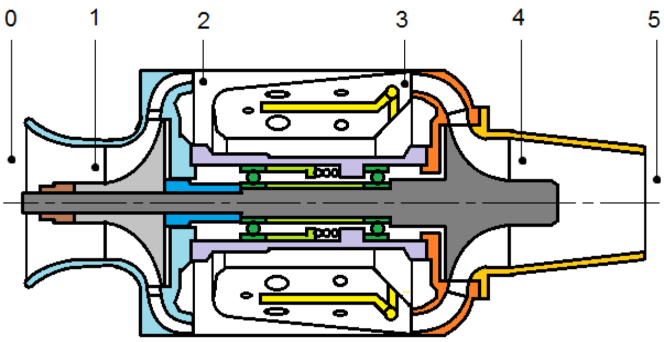

Figure 1 Longitudinal section of a micro turbojet with the annotation of the important aerodynamic stations

2. CONTROL OF TURBOJET ENGINES

2.1. Theoretical background

To understand the necessity of control of turbojet engines one should investigate the equations of balance in mass and energy of the unit. If one considers a single rotor configuration with fixed nozzle exhaust area, neglecting the energy storage capacity of the combustion chamber, there are two continuity equations and one for the conservation of energy through the rotor, as detailed in Equations (1) to (3):

$$\dot{m}_2 + \dot{m}_f - \dot{m}_3 = dm_{CC}/dt \tag{1}$$

$$\dot{m}_4 - \dot{m}_6 = dm_N/dt \tag{2}$$

$$P_T \cdot \eta_m - P_C - P_{off} = 4 \cdot \pi^2 \cdot \Theta \cdot n \cdot dn/dt \tag{3}$$

In the above equations, $\dot{m}$ stands for the mass flow rate at the indicated aerodynamic station, $\dot{m}_f$ is the fuel mass flow rate. On the right sides of Equations (1) and (2) one can identify the elementary change of mass divided by the elementary time difference in the combustion chamber (index CC) and exhaust nozzle (index N), respectively. Equation (3) presents the relationship between turbine power P_T, mechanical efficiency η_m, compressor power P_C, power offtake P_{off}, inertia of the rotor Θ, rotor speed n and acceleration dn / dt.

In some cases, especially for larger constructions and turboshaft configuration, where the exhaust duct is practically a free opening towards the atmosphere, the Equation (2) can be neglected, and there is an additional relationship for the energy storage in the combustion chamber [1]:

$$dU^*_{CC}/dt = \dot{m}_2 \cdot i^*_2 - \dot{m}_3 \cdot i^*_3 + H_c \cdot \eta_c \cdot \dot{m}_f \tag{4}$$

In Eq. (4) the symbol U^*_{CC} denotes the total internal energy of the combustion chamber, i^* stands for the specific total enthalpy at the given aerodynamic station, H_c is the heat of combustion for the fuel, and η_c is the efficiency of the combustion process.

If the above equations are investigated, one can find that the number of included independent variables is more than the number of available equations. There is a need to complete the system of equations with an additional relationship that is the control law. If the nozzle exhaust area is constant, there is a single additional variable and consequently control parameter. In military engines, where thrust augmentation is used, the nozzle must be constructed of a variable geometry, introducing an additional unknown. In the present article the investigation is reduced to the fixed area nozzle.

2.2. Control laws of gas turbine engines

All control systems should allow the pilot to set the thrust proportional to the throttle lever position. Unfortunately, the thrust is not measurable when the engine is installed into the aircraft. Consequently the control of gas turbine engine is always an indirect regulation of other parameters that more or less describe the thrust.

In the first decades of turbojet engines the rotor speed *n* was chosen as the control law. Until the aircraft remains at a low altitude and travels with a moderate subsonic speed, the physical rotor speed delivers a good correlation with thrust developed by the engine. As the flight altitudes and velocities both increased, it became obvious that the corrected speed n_{corr} provides a better approximation, which is defined as follows:

$$n_{corr} = n \Big/ \sqrt{T_1^*} \tag{5}$$

If one considers the operation principle of the turbojet, the thrust is practically the product of mass flow through the engine and the difference of velocities at the exhaust and inlet. As the exhaust gas velocity depends on the nozzle pressure against ambient pressure, measuring total pressures at turbine discharge and compressor inlet (p_4*and p_1*, respectively) leads to the Engine Pressure Ratio (EPR) that is able to determine the thrust developed under the actual conditions:

$$EPR = p_4^* \big/ p_1^* \tag{6}$$

In the past decade Rolls-Royce have introduced a novel solution to monitor the thrust output of a gas turbine engine; especially focusing on high bypass ratio turbofan designs, like RR Trent 1000 [16]. The parameter is called as Turbofan Power Ratio (TPR) and is defined as the product of compressor total pressure ratio and the square root of the overall total temperature ratio of the engine [23]:

$$TPR = p_2^* \big/ p_1^* \cdot \sqrt{T_3^* / T_1^*} \tag{7}$$

In Equation (7), T_3* is the turbine inlet total temperature (TIT), which is rarely measured due to the non-uniform temperature distribution in that location and high temperatures used in up-to-date designs. Although the TIT is typically much lower in micro turbojet engines, here the small dimensions rise difficulties. As a possible solution the turbine discharge temperature, or in other words, the exhaust gas temperature (EGT) T_4* is used instead of T_3* in Eq. (7).

2.3. Control algorithms

Although gas turbine engines exhibit highly non-linear behaviour over the complete range of operation, in most of the cases classical linear algorithms are developed for control. As it is found commonly in all branches of the industry, proportional-integral-derivative (PID) controllers are the most widely spread solutions due to their simplicity [6]. In order to provide the awaited performance over a wide range of operation, the PID systems often use gain scheduling [19]. In the recent decade, there were numerous efforts to realize linear, parameter-varying (LPV) control systems for aviation engines as reported in e.g. [7] and [4]. There were developments for establishing Linear Quadratic Regulator (LQR) for gas turbine engines as well, as it can be found eg in [21]. This approach can be extended with Gaussian distribution disturbance model (LQG) and if the plant is not exactly determinable the Loop Transfer Recovery method (LTR) can be used [9].

Several nonlinear approaches have been developed as well, ranging from fuzzy logic control [5] including sliding mode control (SMC) [13] through H∞ [8] to Nonlinear Model Predictive Control (NMPC) [20]. Rolls-Royce was among the first users of nonlinear inverse model control with the Trent 1000 series engine in 2006 [16].

Novel approaches like situational control have been introduced as they are not only monitoring the command input and manipulate the engine to follow that, but they are able to detect different normal and abnormal conditions which may require diverse strategies to cope with [3]. In this respect, the control system can change to another algorithm as well and all defined situations can be handled with optimum performance, ie there is no burden to solve all problems with a single approach.

In the present work the PID algorithm was selected for the basis of the control system.

3. THE MODULAR CONTROL SYSTEM

3.1. Determining the transfer function of the gas turbine

The PID controller is a serial compensator that receives the difference between the awaited reference signal and the output of the plant to be controlled. This term is called as error, which is fed to the PID controller in order to elaborate an input signal for the plant to reach a zero error state. The general build-up of the system can be found on Fig. 2.

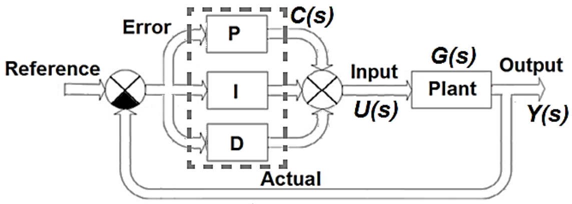

Figure 2 Schematic of PID controlled system

In order to establish such a control system, the transfer function of the plant has to be determined. First of all, this means that the input and output of the system must be specified.

For the turbojet engine, the input is the fuel mass flow rate, but for practical reasons one can choose a more suitable value to reduce the computational requirements. Let us assume that the fuel is supplied by a brushed DC electric motor driven pump and the amount of delivered fuel is changed with the help of pump drive speed control. The speed regulator is a commercial brushed DC motor controller, which requires standard pulse width modulation (PWM) input signals, which is defined in eg [14]. If the battery voltage can be assumed to be constant, the input PWM signal is proportional to the delivered fuel flow, so this is selected for the input of the plant.

The output is the Turbofan Power Ratio defined by Eq. (7), although the present work deals with a turbojet configuration without a fan for the bypass stream. Later in this paper it will be shown that the selected TPR parameter has an excellent correlation with thrust consequently in a turbojet engine it can be utilized as well.

The next step is to determine the transfer function between the selected input and output. This has been realized with several measurements carried out with an automatic feature programmed in the controller under development called "special operation". This provides an increasing frequency square wave input around a specified mean value in order to simulate sinusoid excitation for the plant. The result is a large set of measured values digitized by the controller itself and sent to the data acquisition computer through an RS232 interface. A typical data set is presented on Fig. 3.

The data are sampled at discrete times and due to the analog-digital conversion they are representing discrete values of their respective parameter. The author has created a LabVIEW software in order to evaluate the correlation between the input and output values to determine the transfer function for the discrete system. The Output-Error model has been used, which yielded the following expression shown in Eq. (8).

$$y(k)=\frac{0.00374}{1-1.924\cdot z^{-1}+0.9326\cdot z^{-2}}\cdot u(k)+e(k) \tag{8}$$

The conversion of the discrete system to a continuous one resulted in the transfer function as follows.

$$G(s) = \frac{0.00374 \cdot s^2 + 10.81 \cdot s + 96.87}{s^2 + 3.49 \cdot s + 21.86} \tag{9}$$

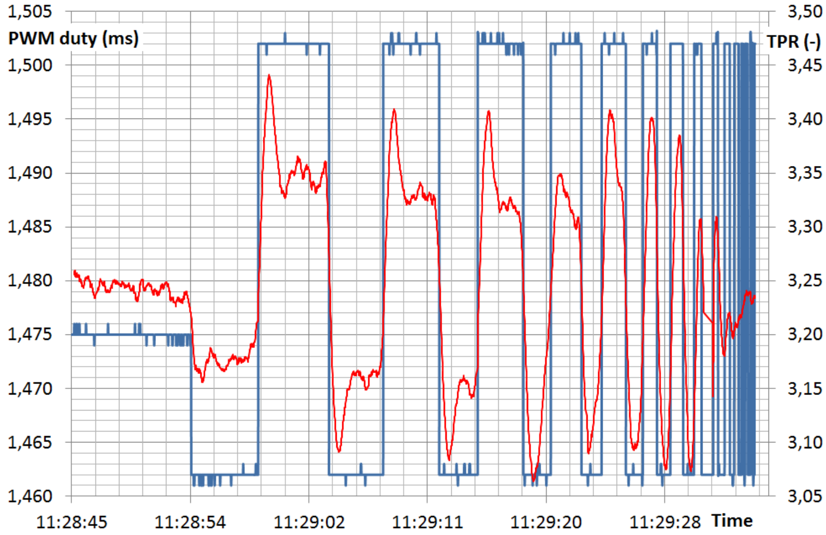

Figure 3 Effect of square wave excitation on TPR

The system description can be reduced if one considers the Bode plot that is shown on Fig. 4. Frequencies over 10Hz are not relevant because in reality the turbojet will not receive such a rapid disturbance. If the higher exponent parts of the numerator are omitted and the single constant is remaining, significant simplification arises while the system response is almost identical to the original model in that frequency range where the operation is assumed (below 10Hz). The original and simplified system Bode plots can be compared on Fig. 4.

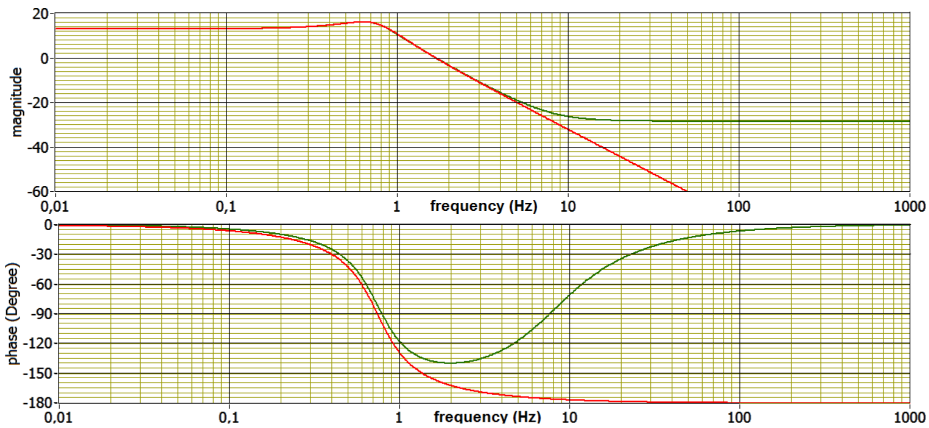

Figure 4 Bode diagram of original (green) and reduced system (red) representation

Introducing the above mentioned reduction, the final transfer function to be used in the subsequent steps is as follows:

$$G(s) = \frac{96.87}{s^2 + 3.49 \cdot s + 21.86} \tag{10}$$

3.2. Establishing the PID control

ISSN 1339-9853 (online), acta-avionica.tuke.sk ISSN 1335-9479 (print) © 2015 LF TUKE

After the transfer function has been acquired, the PID controller can be designed. In the same LabVIEW software, where the previous step was carried out, the optimization of the closed loop control was solved as well. The formula used in the investigation was the equation of parallel connected terms, as it is also shown on Fig. 2:

$$C(s) = K_P + K_I / s + K_D \cdot s \tag{11}$$

Based on an optimization process, the terms of the PID controller were selected as listed in Eq. (12).

$$K_P = 0.090;\ K_I = 0.500;\ K_D = 0.025 \tag{12}$$

The required quality parameters, which were taken into account, were overshoot, response time and settling time. Figure 5 shows the simulated behaviour of the closed loop system response on a step signal.

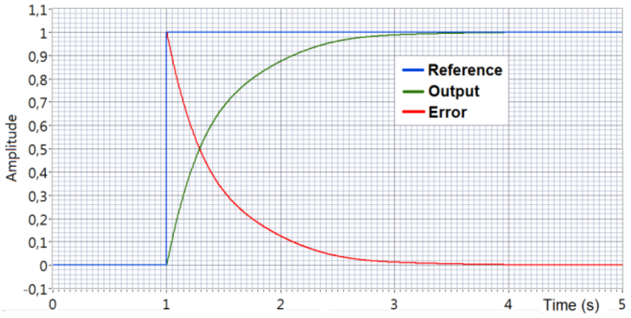

Figure 5 Response of the closed loop system

Fig. 5 shows a step signal applied to the reference (TPR) input. The response of the system shows a smooth transient without oscillation. Evaluating the curves on Fig. 5 one can state that the designed system has fair time domain properties, ie zero overshoot is established with a response time of 1.05 seconds, and settling time of 2.15 seconds, which seems acceptable for a turbojet engine.

3.3. Implementation of the control algorithm

The control algorithm was implemented in an electronic unit, called as Modular Aero-engine Remote Control Electronics (abbreviated as MARCEL) [15]. The previous chapter yielded the Laplace transformed description of the PID controller terms. As the digital control system operates in discrete time, one has to apply an inverse Laplace transform on Eq. (11):

$$u(n) = K_p \cdot e(n) + K_i \cdot \sum_{k=0}^{n} e(k) + K_d \cdot (e(n) - e(n-1)) \tag{13}$$

Here, *e(n)* and *e(n–1)* are the present and most recent errors (difference between reference and actual values), respectively, $\sum_{k=0}^{n} e(k)$ is the sum of errors up to the present time. The coefficients with small letters in the index stands for the values transformed to time domain:

$$K_p = K_P;\ K_i = K_I \cdot T;\ K_d = K_D / T \tag{14}$$

In Eq. (14) the *T* symbol stands for the cycle time of the controller's main loop. The main processor of the FADEC contains a real time counter that is able to generate interrupts. This has been set to raise ten interrupts every second, ie the time constant is 100 milliseconds. This was proven during the test satisfactory, however, as others like [13] have stated, up-to-date systems operate around ten times faster, so that is a natural goal of the present research as well.

As it has been reported previously in a former stage of the development in [15], the control system is based on a modular concept with an Freescale (former Motorola) MC9S08DN60 microcontroller that features 8-bit architecture, 60kB program memory, 4kB RAM, 12 bit successive approximation analog-digital converter, and 6 channels of 16 bit timer.

The implementation of the PID algorithm includes the manipulation of the sum for the integral term. This is defined as a two byte signed integer, with a range between [–32768…+32767]. Therefore an important feature is to prevent accidental wraparound when there is an unhandled overflow in this variable. The limits of turbojet engine operation required a useful range of [–9000…+32000] this means larger sum than the included would overdrive the input of the fuel pump resulting in insufficient or abnormally high delivery, which both are unacceptable.

The modularity of the FADEC system means that the major functions are realized on different printed circuit boards (PCB's). For the inevitable ground tests there are several features which will not be used during a flight. The general overview is shown on Fig. 6.

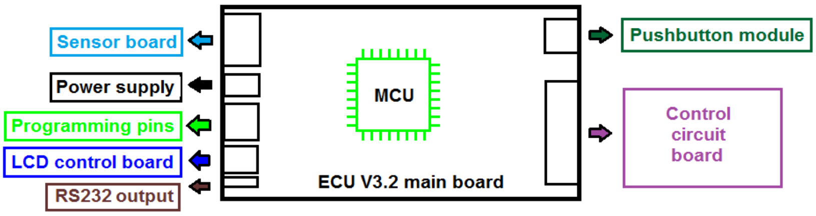

Figure 6 Overview of MARCEL V3.2

For example, the RS232 communication with an external computer for data acquisition is limited to the ground operations. The controller is equipped with an LCD for real time (volatile) indication on the controller box itself if the computer is not available, and there are pushbuttons to navigate through the menu system on the LCD. The sensor board includes such devices that allow the deeper understanding of the gas turbine operational process, eg additional temperatures and pressures, but are not essential for the control consequently they would be surplus during flight. This is the reason why the modular design was chosen, because the main board contains all the necessary components to realize the control and its weight and dimensions were kept at a reasonable minimum to meet the requirements of the aircraft. The following figures show the bare PCB's (Fig. 7) and the main screen of the controller during operation (Fig. 8).

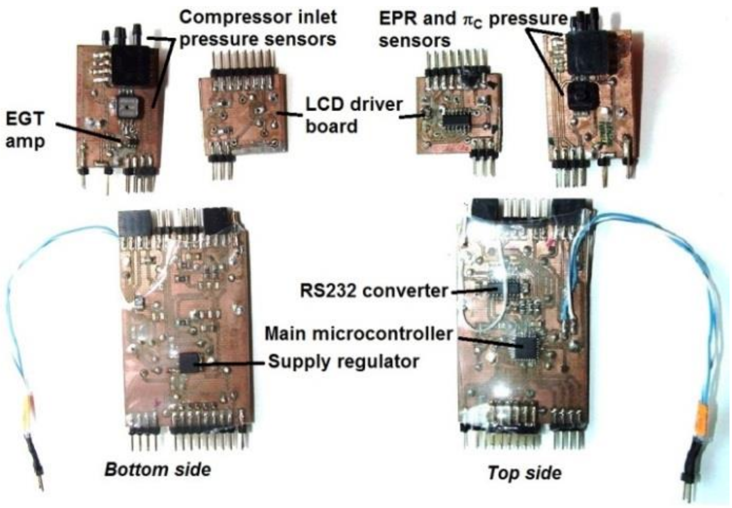

Figure 7 Printed circuit boards of MARCEL

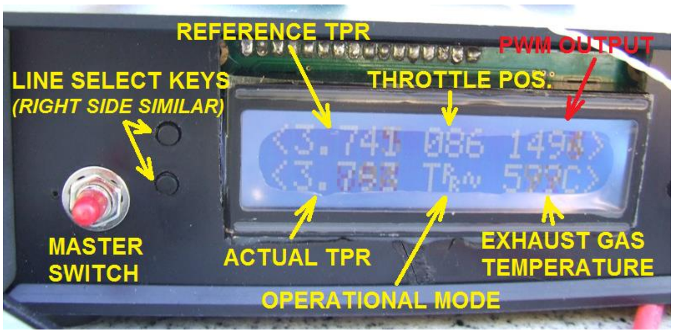

Figure 8 LCD screen during operation

4. INVESTIGATION OF THE CONTROLLER

4.1. Adjusting the PID gains

The automatic design of the PID controller has resulted in the above mentioned gains of the individual terms, but the implementation has resulted in overfueling during extreme throttle movement, ie moving the throttle lever from idle to maximum within a single 1/10 second which is equal to the sampling time of the controller. As the FADEC includes the ability to adjust the gains real-time during operation, with the LCD interface it was possible to set the correct value. It has been found that the proportional gain decreased from its original value of 0.09 down to 0.05 has solved the problem and resulted in a smooth acceleration even with the most extreme throttle movement. It has to be noted, that the design of the controller was based on measurements in the TPR range of 2.6…3.5. This corresponds a 66…90% of the nominal rotor speed, meanwhile idle TPR is approximately 2.0, ie it is far enough from the operational point where the nonlinearity of the plant can result in such deterioration of the performance.

4.2. Investigation of the controller behaviour

After determining the gains for the whole operational range, the engine was run to collect information from idle to the maximal. For an extended evaluation, the idle speed has been reduced to investigate the behaviour under adverse conditions, ie when an unpredictable disturbance drives the system under the idle speed.

Figure 9 (right side) presents the period near to start of a complete operation. One can identify the initial pre-heating of the combustion chamber, in order to produce hot environment enabling the evaporation of the incoming fuel. After approximately five seconds after the initialization, the throttle has been increased to the level that corresponds the preliminary supply for the correct lightoff condition. Until the fuel is ignited a small increase in rotor speed can be measured; as the lightoff is established the acceleration due to the turbine power is more emphasized (between 5 and 10 seconds after start). At 10 seconds after start, the TPR reaches the idle value and the PID takes over the control from the predetermined acceleration logic. Here it is clear that the turbojet has significantly different behaviour near to idle (approx. 50% of the nominal rotor speed, ie 60 krpm) consequently the determined gains do not lead to a stable, aperiodic operation. Meanwhile, the higher EGT is also an additional contributor to this effect. After the rotor speed is increased to near 80 krpm (66%), the control is able to hold the selected TPR reference within 1%.

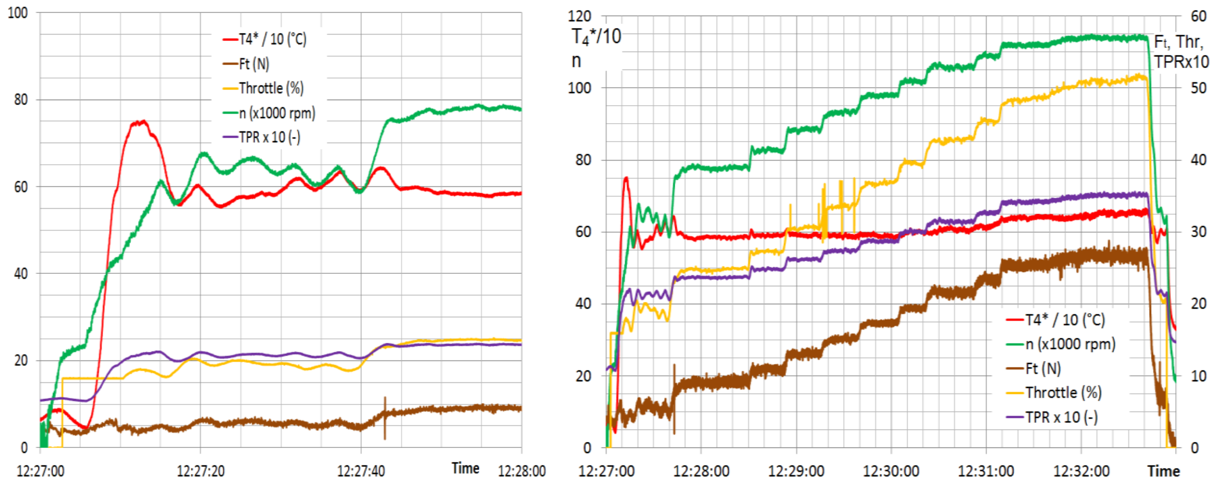

Figure 9 Operation during start and near to idle (left) and complete operation cycle (right)

Figure 9 (left side) shows the complete operation from start to almost the maximum speed (114 krpm, 95% of nominal). The reference was increased in steps after establishing a stable operation at TPR equal to 2.375, as described above. The steps were approximately ΔTPR = 0.125, and the time spent at each level was near to 20 seconds in order to allow the engine to reach the stable operational condition. It is obvious from Fig. 10 that above half of the nominal speed the control system produces a smooth transient from one setpoint to another and fair, stable steady-state operation as well. It can be also seen that some significant noise has been recorded on the throttle channel between times 12:29 and 12:30 as the setpoint has been changed from 30 to around 33%. This information is measured in a different way, ie instead of proportional voltage to be converted to digital value it is a time value of a pulse width modulation signal duty cycle that has to be measured with a counter. Therefore these glitches are considered as nuisance readings of the data acquisition module.

Figure 10 contains detailed timelines of the four major parameters showing a selected operational mode at approximately 70% of the nominal speed. It can be seen that after some decaying oscillation the TPR catches the selected reference and remains within 1% of that value.

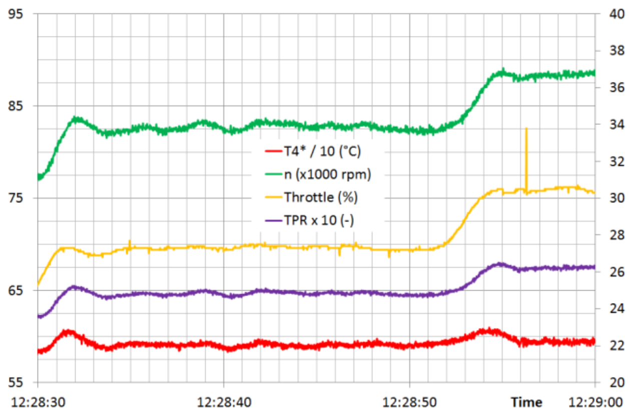

Figure 10 Transient operation

On Fig. 11 one can evaluate the relative deviation from the selected reference of the same timeline. The peak values in both positive and negative direction are approximately 1% of the nominal, as stated above. The mean value of the error is 0.373% using the least squares method.

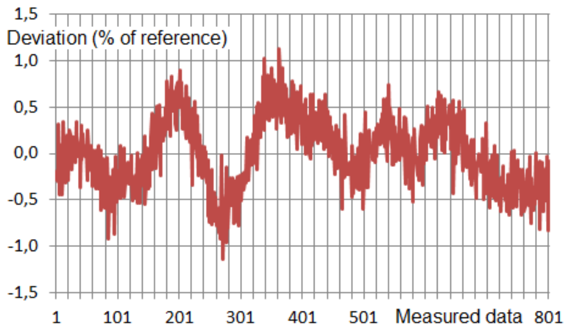

Figure 11 Deviation from reference (steady-state operation)

4.3. Correlation between TPR and thrust

It is an important role of the present investigation to deliver the correlation between TPR and thrust because the former parameter was originally intended to describe the thrust developed by a high bypass ratio turbofan engine, meanwhile here the utilization in a turbojet was considered. The collected large number of operational data made it possible to evaluate this relationship as well.

As it can be foreseen, the TPR, although developed for turbofans, does not contain any relevant factor that is exclusively applicable to turbofans only. Therefore the possibility of usage in the control system for a turbojet was considered to have a fair chance.

Regarding to the previously detailed charts, TPR is an applicable basis for the control, but another question is the relationship between TPR and thrust. Collecting all data (including transient operational circumstances as well) the two parameters are shown plotted against each other. A linear trend line was set which refers to the average of the measurements.

Because during the normal engine operation the temperature ratio in Eq. (7) is always much larger than unity, despite the possibly negligible compressor pressure ratio at idle TPR is around 2 also when there is practically no thrust output. As an additional information, the compressor pressure ratio at idle is 1.2, while at the nominal speed it increases to 2.4.

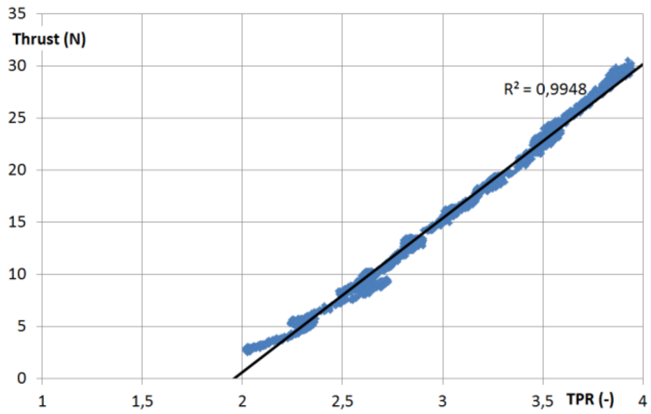

Figure 12 Correlation of TPR and thrust

Here it should be noted that the measurements were conducted using a still standing turbine test bench. That means the correlation between the two investigated parameters inflight, when the incoming air velocity significantly modifies the circumstances, should be investigated later.

As a conclusion to Fig. 13 one can state that there is an exact and useable correlation between TPR and thrust, so that the former can be applied as a thrust parameter for turbojet engines as well.

5. CONCLUSION

5.1. Realized goals

The present article showed the design of a modular control system for micro scale turbojet engines from the initial concepts through the establishing of the PID control to the measurements carried out with the realized hardware.

It was shown that a proportional-integral-derivative serial compensation controller can be designed for such a highly nonlinear system with a simplified approach to determine the system's transfer function in selected operational points and then create a control which will be applicable for these regimes.

The author has realized the hardware for the FADEC with the predetermined modular concept that makes it suitable for thorough ground tests as well as for inflight duty. The controller includes additional features like fault detection and isolation, two-ways communication with the user through a real-time LCD indication and pushbutton array, RS232 communication with a data acquisition computer for collecting and offline evaluating the data generated during an engine run.

There were extended test runs of the controller in the whole range of the gas turbine engine in order to confirm correct operation of the coupled system. Except for an isolated range near to idle the controller proved the required quality is met.

The TPR was originally intended to be used in control systems for turbofan engines, and nowadays it is only used to override the original low pressure rotor speed regulation. This article had two major goals in this aspect:

1. To show the TPR is able to be used as the basic thrust parameter regardless of any other engine parameters. This investigation proved that TPR-based control is possible and realizable.
2. To show there is an exact correlation between TPR and thrust. During the measurements, the thrust against TPR has been collected and plotted in a chart showing an excellent correlation between the two parameters even in the case of the turbojet utilization. One can draw the conclusion: the TPR can be used also in the field of turbojet engines.

5.2. Further developments

Naturally, one can find some aspects, where the present research has not reached a goal, due to difficulties or restrictions in the project. This gives a variety of further developments that are briefly considered hereafter.

The control algorithm used in the MARCEL system is the most basic PID with fixed gains. First, with a relatively small effort a gain scheduling variant can be realized. As a next step, different algorithms can be investigated as well.

The modular controller hardware has shown some points where corrections can result in more optimal arrangement and further reduction of both weight and dimensions. The firmware is now missing the possibility of handling a non-volatile memory, which can significantly extend the features of the system by storing operational time, faults, etc. Although the controller is sending measured data through an RS232 line, the receiver function must be implemented as well.

The controller was tested in ground operational conditions. In flight, there are always different circumstances due to the velocity effects. Therefore, the whole system should be investigated when it is installed on an aircraft in the possible widest operational range considering flight altitude and Mach number.

Finally, after conducting the previously mentioned tests, the system can be developed further to give the possibility for autothrust as well.

6. LITERATURE LIST

Journals:

[1] Ailer, P. - Sánta, I. - Szederkényi, G. - Hangos, K. M.: Nonlinear Model-Building of a Low-Power Gas Turbine. *Periodica Polytechnica Ser. Transp. Eng*. ISSN 1587-3811, Vol. 29, No. 1-2, pp. 117–135 (2001)

[2] Amirante, R., et al. Design optimization of the intake of a small-scale turbojet engine. *Computer Modelling in Engineering and Sciences*, 2007, vol. 18, no. 1, pp. 17-30. ISSN: 1526-1492 doi:10.3970/cmes.2007.018.017

[3] Andoga, R. - Madarász, L. - Főző, L. - Lazar, T. - Gašpar, V.: Innovative approaches in modeling, control and diagnostics of small turbojet engines. *Acta Polytechnica Hungarica*. Vol. 10, no. 5 (2013), p. 81-99. - ISSN 1785-8860. Available from: http://www.uni-obuda.hu/journal/Andoga_Madarasz_Fozo_Lazar_Gaspar_43.pdf [cited 2015-02-28]

[4] Balas, G. Linear, parameter-varying control and its application to a turbofan engine. *International Journal of Robust and Nonlinear Control*, 2002, Vol. 12, No. 9, pp. 763-796. ISSN: 1099-1239 doi: 10.1002/rnc.704

[5] Bazazzadeh, M. - Badihi, H. - Shahriari, A. Gas Turbine Engine Control Design Using Fuzzy Logic and Neural Networks, *International Journal of Aerospace Engineering*, Volume 2011, pp. 12, doi:10.1155/2011/156796

[6] Dhiman, P. et al. Review on Exhaust Temperature Control of Gas Turbine. *International Journal of Engineering and Innovative Technology*. 2013, Vol. 2, No. 9, pp. 260-264. ISSN 2277-3754.

[7] Gilbert, W. - Henrion, D. - Bernussou, J. - Boyer, D. Polynomial LPV synthesis applied to turbofan engines. *Control Engineering Practice*, 2010, Vol. 18, No. 9, pp. 1077-1083. ISSN: 0967-0661 DOI: 10.1016/j.conengprac.2008.10.019

[8] Härefors, M. Application of H∞ robust control to the RM12 jet engine. *Control Engineering Practice*, 1997, Vol. 5, No. 9, pp. 1189-1201. ISSN: 0967-0661 DOI: 10.1016/S0967-0661(97)84358-4

[9] Shabaninia, F. - Jafari, K. Using LQG/LTR Optimal Control Method to Improve Stability and Performance of Industrial Gas Turbine System. *International Scholarly Research Network (ISRN Electronics)*, Volume 2012, pp. 8, doi:10.5402/2012/134580

Books:

[10] Főző, L., Andoga, R., and Madarász, L.: Mathematical Model of a Small Turbojet Engine MPM-20. In: *Studies in Computational Intelligence*. Edited by Rudas, I. – Fodor, J. Vol. 313 (2010), pp. 313-322. ISBN 978-3-642-15220-7, doi: 10.1007/978-3-642-15220-7_25, p. 348.

[11] Kamps, Thomas: Model Jet Engines. Traplet Publication Ltd., 3rd edition, 2005., p. 109.

[12] Nascimento, M. A. R., et al. Micro Gas Turbine Engine: A Review. In: *Progress in Gas Turbine Performance*, edited by Dr. Ernesto Benini, 2013, ISBN: 978-953-51-1166-5, InTech, DOI: 10.5772/54444. Available from: http://www.intechopen.com/books/progress-in-gas-turbine-performance/micro-gas-turbine-engine-a-review [cited 2015-02-28]

[13] Richter, H. *Advanced Control of Turbofan Engines*. New York: Springer, 2012. p. 266. ISBN 978-1-4614-1170-3. DOI 10.1007/978-1-4614-1171-0

Conference Proceedings:

[14] Behnke, S. - Schreiber, M. Digital Position Control for Analog Servos. In: *Proceedings of the Workshop on Humanoid Soccer Robots of the 2006 IEEE-RAS International Conference on Humanoid Robots*, 2006, ISBN 88-900426-2-1, pp. 56-61. Available from: http://www.dei.unipd.it/~emg/whs2006/papers/HSR-111.pdf [cited 2015-02-28]

[15] Beneda, K. Modular Electronic Control for Small Scale Turbojet Engine. In: *Proceedings of the International Scientific Conference New Trends in Aviation Development 2014*, ISBN 978-80-553-1650-5

[16] Davies, C. - Holt, J. E. - Griffin, I. A. Benefits of inverse model control of Rolls-Royce civil gas turbines. In: *International Control Conference*. Glasgow, University of Strathclyde, 2006. pp. 70-76. ISBN 0 974649549 [cited 2015-02-28] Available from: http://ukacc.group.shef.ac.uk/proceedings/control2006/papers/f70.pdf

[17] Katolický, Z. - Bušov, B. - Bartlová, M. Turbojet engine innovation and TRIZ. *16th International Conference on Mechatronic*, pp. 16-23, 3-5 Dec. 2014. doi: 10.1109/MECHATRONIKA.2014.7018230

[18] Matsunuma, Takayuki, et al.: Micro Gas Turbine with Ceramic Nozzle and Rotor. In: *ASME Turbo Expo 2005: Power for Land, Sea, and Air*, ISBN: 0-7918-4699-7., pp. 973-979; doi:10.1115/GT2005-68711

[19] Mu, J. - Rees, D. - Chiras, N. Optimum Gain-Scheduling PID Controllers for Gas Turbine Engines Based on NARMAX and Neural Network Models. In: *Proceedings of ASME Turbo Expo*, ASME, 2003. pp. 509-515, ISBN: 0-7918-3684-3, doi:10.1115/GT2003-38667

[20] Mu, J. - Rees, D. Approximate Model Predictive Control for Gas Turbine Engines. In: *Proceedings of the American Control Conference*, American Automatic Control Council, 2004. pp. 5704-5709. ISBN 0-7803-8335-4.

[21] Richman, M. - Gordon, V. Improved gas turbine response using LQR control. In: *Symp. Design Principles and Methods for Aircraft Gas Turbine Engines*, RTO MP-8, Toulouse, France. 1998. p. 11-15. [cited 2014-07-04] Available from: http://ftp.rta.nato.int/Public/PubFullText/RTO/MP/RTO-MP-008/$MP-008-16.pdf

[22] Verstraete, Dries, et al. Micro propulsion activities at the University of Sydney. In: *Proceedings of the PowerMEMS 2010 Conference*. 2010, pp. 255-258. Available from: http://cap.ee.ic.ac.uk/~pdm97/powermems/2010/poster-pdfs/255_Verstraete_41.pdf [cited 2015-02-28]

Web sites:

[23] Rowe, A. L. - Kurz, N. *Control System for a Ducted Fan Gas Turbine Engine*. United States Patent No. 5887419, 1999, [cited 2015-02-28] Available from: http://patentimages.storage.googleapis.com/pdfs/US5887419.pdf